LAWRENCE
LIVERMORE
NATIONAL
LABORATORY

LLNL-JRNL-750006

# Velocity correction for nuclear activation detectors at the NIF

H. Rinderknecht, R. Bionta, G. Grim, R. Hatarik, H. Khater, C. Yeamans

April 23, 2018

Review of Scientific Instruments

## Disclaimer

This document was prepared as an account of work sponsored by an agency of the United States government. Neither the United States government nor Lawrence Livermore National Security, LLC, nor any of their employees makes any warranty, expressed or implied, or assumes any legal liability or responsibility for the accuracy, completeness, or usefulness of any information, apparatus, product, or process disclosed, or represents that its use would not infringe privately owned rights. Reference herein to any specific commercial product, process, or service by trade name, trademark, manufacturer, or otherwise does not necessarily constitute or imply its endorsement, recommendation, or favoring by the United States government or Lawrence Livermore National Security, LLC. The views and opinions of authors expressed herein do not necessarily state or reflect those of the United States government or Lawrence Livermore National Security, LLC, and shall not be used for advertising or product endorsement purposes.

# Velocity correction for neutron activation diagnostics at the NIF

Hans G. Rinderknecht,[a] R. Bionta, G. Grim, R. Hatarik, H. Khater, D. Schlossberg, and C. Yeamans
*Lawrence Livermore National Laboratory, Livermore, California 94550, USA*

(Presented 16 April 2018; received 4 May 2018; accepted 25 May 2018; published online 10 October 2018)

The velocity distribution of the hotspot in an inertial confinement fusion implosion changes the energy spectra of fusion neutrons emitted from the experiment as a function of viewing angle. These velocity-induced spectral changes affect the response of neutron activation diagnostics (NADs) positioned around the experiment and must be accounted for to correctly extract information about areal density ($\rho R$) asymmetry from the data. Three mechanisms through which average hotspot velocity affects NAD activation are addressed: change in activation cross section due to the Doppler shift of the mean neutron energy, kinematic focusing of neutron fluence, and change in the scattering cross section due to the Doppler shift. Using the hotspot velocity inferred from neutron time-of-flight measurements of D-T and D-D fusion neutrons, the hotspot velocity is shown to account for the observed NAD activation asymmetry in a calibration shot with negligible fuel $\rho R$. A robust method to evaluate uncertainties in spherical-harmonic fits to the NAD data due to the velocity correction and detector uncertainty is discussed. *Published by AIP Publishing.* https://doi.org/10.1063/1.5038734

## I. INTRODUCTION

In Inertial Confinement Fusion (ICF) implosions, the symmetry of the assembled hotspot and cold deuterium-tritium fuel is of fundamental importance to attaining ignition and burn. Asymmetries imply inefficiencies in fuel compression and are currently thought to be a primary source of the underperformance of experiments at the National Ignition Facility (NIF) as compared to theoretical predictions.[1] The neutron activation diagnostic (NAD) suite at the NIF is sensitive to variations in neutron fluence with detection angle, which are produced by asymmetries in the areal density ($\rho R$) of the assembled cold fuel.[2] In addition to neutron scattering, activation detectors are affected by other systematic changes to the neutron spectrum, including Doppler shifts in the spectrum due to mean hotspot velocity. Previously this sensitivity has been used to infer the hotspot velocity from NAD data on shots with negligible fuel $\rho R$.[3] Large mean hotspot velocities and areal density perturbations can both be produced in ICF implosions by mode-1 drive asymmetries.[4] To accurately assess the cold fuel symmetry in cryogenic implosions, the contribution of velocity to the observed activation asymmetry must be removed.

This manuscript presents the technique for correcting NAD activation data for an inferred mean hotspot velocity and an application of this technique to a shot with a strong imposed mode-1 drive asymmetry. Section II discusses three ways in which mean velocity affects the activation diagnostics and derives the scaling for each effect. Section III describes the method used for inferring a mean hotspot velocity from the neutron Time-of-Flight (NTOF) detectors at the NIF and the appropriate method for propagating uncertainties from the inferred velocity to the activation correction. Section IV presents the results of applying this technique to a low areal density implosion with a large drive asymmetry, and Sec. V concludes.

## II. ACTIVATION CORRECTIONS WITH VELOCITY

In the zirconium-90 activation diagnostics used at the NIF, the detector activation $A$ after exposure to a neutron fluence $F$ (neutrons/cm$^2$) is determined by an integral over the neutron spectrum ($dF/dE$),

$$A = N_{Zr} \int \sigma_{Zr,n} \frac{dF}{dE} dE, \tag{1}$$

where $N_{Zr}$ is the number of zirconium-90 atoms in the sample and $\sigma_{Zr,n}$ is the cross section for activation by neutrons, which is a function of neutron energy. The cross section for the reaction of interest, $^{90}$Zr($n$, $2n$)$^{89}$Zr, is plotted in Fig. 1 along with a typical neutron spectrum produced by deuterium-tritium fusion.[5] This cross section has a lower threshold of approximately 12 MeV and increases across the region of interest (~14 MeV) with an approximate linear slope of 0.30 barns/MeV. The signal of interest is variation in activation with detector position caused by variation in areal density, which affects line-of-sight neutron fluence by an associated change in neutron scattering. To assess activation changes with viewing angle, the activation data are generally normalized to a mean value. However, the normalized activation remains sensitive to additional physics that produces variations in the neutron spectrum with viewing angle. A mean hotspot velocity introduces mode-1 variation in neutron energy and fluence with viewing angle, which in turn imprints on the activation distribution.[6] The following evaluates the impact of hotspot velocity on the recorded activation distribution and presents the

Note: Paper published as part of the Proceedings of the 22nd Topical Conference on High-Temperature Plasma Diagnostics, San Diego, California, April 2018.
[a]rinderknecht1@llnl.gov

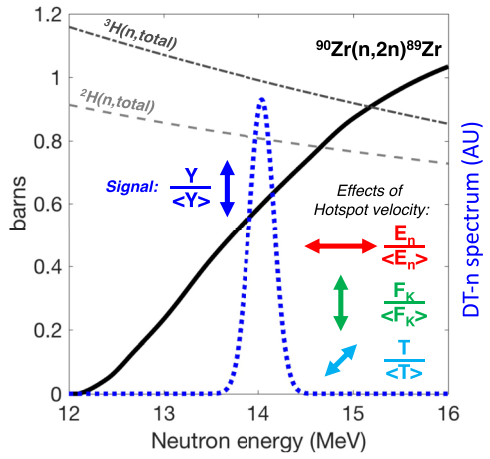


FIG. 1. Neutron activation cross section for the reaction $^{90}$Zr(n,2n)$^{89}$Zr (solid) used to record DT-neutron fluence and neutron scattering cross sections with tritium (dotted-dashed) and deuterium (dashed). A characteristic DT-neutron fusion spectrum (blue dotted) is included for reference. The zirconium activation signal of interest is variation in the peak amplitude due to scattering, $Y/\langle Y\rangle$. Hotspot velocity additionally changes the neutron spectrum, and thus the activation signal, by three effects described in the following sections: change in mean neutron energy, $E_n/\langle E_n\rangle$ (Sec. II A); kinematic change in fluence, $F_K/\langle F_K\rangle$ (Sec. II B); and change in scattering cross section, $T/\langle T\rangle$ (Sec. II C).

technique for renormalizing the activation data to account for these effects and uncovering the residual impact of areal density asymmetry.

### A. Mean neutron energy effect

Net flow of a fusing plasma relative to the detection system introduces a Doppler shift to the fusion products. A neutron produced with velocity $\beta_{n0} = v_{n0}/c$ in the plasma frame will be observed with a velocity

$$\beta_n = \frac{\beta_{n0} + \beta_{HS}\cos\theta}{1 + \beta_{n0}\beta_{HS}\cos\theta}, \tag{2}$$

where $\beta_{HS}$ is the residual hotspot velocity and $\theta = \cos^{-1}\left(\vec{\beta}_{n0}\cdot\vec{\beta}_{HS}\right)$ is the angle between the direction of the hotspot flow and of the detector. The kinetic energy in the detector frame is given by the formula $E_n = (\gamma_n - 1)M_n c^2$, where $M_n$ is the neutron mass and $\gamma_n = \left(1-\beta_n^2\right)^{-1/2}$. Taking advantage of the relative slowness of residual hotspot velocities ($\beta_{HS} \lesssim 0.001 \ll \beta_{n0} \sim 0.17$), the relativistic energy formula may be expanded to first order in $\beta_{HS}/\beta_{n0}$ to obtain the energy shift $\Delta E = (E_n - E_0)$ due to hotspot velocity as

$$\Delta E \approx E_0 \frac{\beta_{HS}}{\beta_{n0}}\cos\theta\left[\frac{\beta_{n0}^2\left(1+\beta_{n0}^2\right)}{\left(1-\beta_{n0}^2\right)\left(1-\sqrt{1-\beta_{n0}^2}\right)}\right]. \tag{3}$$

Given the approximate symmetry of the fusion neutron peak, which is well described as a Gaussian with mean energy $\langle E\rangle$ and spectral width $\sigma_E$,[7] $\Delta E$ may be taken as a systematic shift in the neutron energy due to hotspot velocity as a function of viewing angle $\theta$. For a typical mean neutron energy $\langle E\rangle$ = 14.1 MeV, the term in square brackets in Eq. (3) has a value of approximately 2.11. Combining this formula with the slope of the activation cross section around this energy and the mean activation cross section ($\langle\sigma\rangle$ = 0.6 barns), the total change in activation due to the Doppler shift in neutron energy is derived to be $A/\langle A\rangle = \sigma/\langle\sigma\rangle \approx 1 + 14.4(\beta_{HS}/\beta_{n0})\cos\theta$. The activation shift due to the Doppler shift from a 100 km/s hotspot flow is approximately 2.8% cos $\theta$.

### B. Kinematic focusing effect

A net flow of plasma relative to the detection system also introduces a kinematic focusing, in which greater neutron fluence is produced in the direction of flow. In the rest frame of the fusing plasma, neutrons are equally likely to travel in any direction: the probability distribution $P(\Omega')$ for a neutron to go into solid angle $\Omega'$ is $P(\Omega')d\Omega' = d\Omega'/4\pi$. Decomposing the solid angle into polar and azimuthal components ($d\Omega' = \sin\theta' d\theta' d\phi'$) and assuming azimuthal symmetry relative to an angle of interest $\theta'$, this may be rewritten as $P(\theta')d\theta' = (\sin\theta' d\theta')/2$. Transforming into the detector frame, the angle $\theta$ between the detector and the flow direction is given by

$$\tan\theta = \frac{v_r}{v_z + V_{HS}} = \frac{\sin\theta'}{\cos\theta' + \delta}, \tag{4}$$

where $(v_r, v_z) = v_{n0}(\sin\theta', \cos\theta')$ are the components of the neutron velocity in the rest frame and $\delta \equiv V_{HS}/v_{n0}$. Solving this equation for $\cos\theta'$ and calculating the derivative, the probability distribution may be rewritten in terms of the laboratory angle $\theta$,

$$P(\theta) = 2\delta\cos\theta + \sqrt{1-\delta^2\sin^2\theta} + \frac{\delta^2\cos^2\theta}{\sqrt{1-\delta^2\sin^2\theta}}. \tag{5}$$

Figure 2 plots the normalized probability distribution $[P(\theta,\delta)/P(\theta,0)]$ for various hotspot velocities. In the limit $\delta \ll 1$, the first term dominates, and the kinematic focusing effect is reasonably described as a $\cos\theta$ curve that amplifies the fluence in the direction of flow and reduces it in the opposite direction.

On the NIF, individual NAD samples cover a sufficiently small angle ($\Delta\theta \sim 0.7°$) that we may approximate

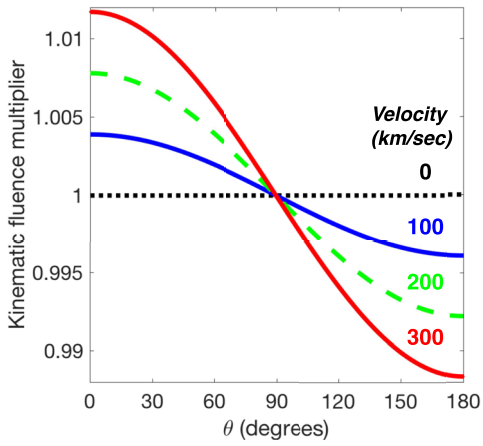


FIG. 2. Change in neutron fluence due to kinematic focusing as a function of detection angle $\theta$ relative to the direction of the hotspot flow; hotspot velocities of 0 (black dotted), 100 (blue), 200 (green dashed), and 300 km/s (red) are shown.

neutron fluence as $F(\theta) = Y\,P(\theta)/(4\pi R^2)$. The total effect of kinematic focusing on activation is therefore derived to be $A/\langle A\rangle = F_K/\langle F_k\rangle \approx 1 + 2(\beta_{HS}/\beta_{n0})\cos\,\theta$. The activation shift due to kinematic focusing from a 100 km/s hotspot flow is approximately 0.4% $\cos\theta$, in the same direction as the energy shift effect but with one seventh of its magnitude.

### C. Scattering cross section effect

The shift in neutron energy due to the hotspot velocity calculated previously will affect not only the probability of activation but also the probability of neutron scattering. Figure 1 shows the tabulated total cross section for neutron scattering with deuterium and tritium near the DT-neutron mean energy.[5] The slope of the (n, d) and (n, t) scattering cross sections near the DT-neutron mean energy is −0.044 and −0.075 barns/MeV, respectively. While these are substantially flatter than the $^{90}$Zr scattering cross section discussed previously, the reduced cross section with increased energy will lead to less scattering (and thus increased fluence) for a given areal density in the direction of velocity and energy upshift. The neutron transmission $T = \exp(-\rho R\sigma_{DT}/M_{DT})$, where $\rho R$ is the areal density of the fuel, $M_{DT} = f_D(2\text{ amu}) + f_T(3\text{ amu})$ is the average ion mass of the fuel, and $\sigma_{DT} = f_D\sigma_{(n,D)} + f_T\sigma_{(n,T)}$ is the concentration-normalized scattering cross section. The change in transmission with detector angle is given by the ratio

$$\frac{T}{\langle T\rangle} = \exp\left[\frac{\langle\rho R\rangle\sigma_{DT}(\langle E\rangle) - \rho R\sigma_{DT}(E)}{M_{DT}}\right], \tag{6}$$

where the bracketed quantities are averaged over all detection angles. The angular dependence of the term $\rho R$ is ultimately the signal of interest; however, to assess the magnitude of the velocity effect on the scattering cross section, this term is assumed here to be constant. Expanding Eq. (6) in small energy shifts $\Delta E/E_0 \ll 1$, a scaling for the transmission is obtained in terms of the hotspot velocity, $T/\langle T\rangle = \exp[(\langle\rho R\rangle\langle\sigma_{DT}\rangle/M_{DT})(\Delta E/E_0)]$. The fraction in parentheses has a value of approximately 0.215 $\langle\rho R\rangle$/(1 g/cm$^2$). Assuming that all scattered neutrons are lost from the detector viewing that angle, the fluence of neutrons along that angle scales with the transmission. Using the result of the prior energy scaling calculation, the scaling of activation may then be approximated as $A/\langle A\rangle = T/\langle T\rangle \approx \exp\left[0.453(\beta_{HS}/\beta_{n0})\cos\,\theta\langle\rho R\rangle/(1\,\text{g/cm}^{-2})\right]$. Typical fuel areal densities are less than or comparable to 1 g/cm$^2$, so the exponential term is small and may be approximated linearly. The activation shift due to change in the neutron scattering cross sections from a 100 km/s hotspot flow is 0.09%[$\langle\rho R\rangle$/(1 g/cm$^{-2}$)] $\cos\theta$. This correction is again in the same direction as the other two corrections; however, the magnitude is comparatively small: only 1/32× the correction due to the energy shift.

### D. Total correction

The three effects considered—changes in activation and scattering due to neutron Doppler shift and kinematic focusing—all contribute to a mode-1 activation pattern that is maximized in the direction of the hotspot flow. By renormalizing the recorded activation data, the effects due to hotspot flow can be removed, leaving only residual effects including the desired areal density anisotropy. The kinematic focusing and scattering effects both scale the background neutron fluence, w hereas t he e nergy s hift s cales t he effective activation cross section. Taking all known effects into account, the observed ratio of activation to mean activation is

$$\frac{A}{\langle A\rangle} = \frac{\int \sigma\frac{dF}{dE}dE}{\int \sigma\frac{d\langle F\rangle}{dE}dE} \approx \frac{Y}{\langle Y\rangle}\frac{\sigma(E)}{\sigma(\langle E\rangle)}\frac{F_K}{\langle F_K\rangle}\frac{T}{\langle T\rangle}, \tag{7}$$

where $Y$ indicates the residual activation due to unscattered neutrons, which is inversely proportional to areal density, and the other effects were calculated earlier. If the hotspot velocity is known, the activation anisotropy due to these effects may be individually estimated and the activation data may be renormalized to define the metric $Y/\langle Y\rangle$ containing only the desired anisotropy in activation due to scattering effects.

## III. VELOCITY INFERENCE AND ERROR PROPAGATION

An accurate, independent measurement of the neutron-averaged hotspot velocity is needed to perform this correction of the NAD data. The neutron time-of-flight (NTOF) diagnostic suite at the NIF[8,9] presently includes four neutron spectrometers positioned at various angles around the implosion: SPEC-NP ($\theta$ = 18°, $\phi$ = 304° in NIF target chamber coordinates), SPEC-E (90°, 175°), SPEC-A (115°, 319°), and SPEC-SP (161°, 57°). In addition to inferring the neutron yield, burn-averaged temperature, and downscattered ratio,[10] these detectors are capable of accurately measuring the Doppler shift of both the DT- and DD-neutron peaks, thereby constraining the projected hotspot velocity $\langle V\rangle$ with a typical uncertainty of ±14 km/s.[11] Given the near transparency of the target to neutrons, all measurements of burn-averaged velocity (including effects on NTOF and NADs) will be sensitive to the entire neutron producing region, and the same net velocity vector $\vec{V}_{HS}$ will cause the inferred velocity effects for all detectors.[12] This vector is obtained by fitting to the measured NTOF velocities. Defining the chi-square metric as

$$\chi^2 \equiv \sum_i^N \frac{\left(\vec{V}_{HS}\cdot\hat{r}_i - V_i\right)^2}{\sigma_i^2}, \tag{8}$$

where $\hat{r}_i$ is the unit-vector direction of the detector and $\sigma_i$ is the uncertainty for each measurement of the projected hotspot velocity $V_i$, the value of $\vec{V}_{HS}$ that minimizes $\chi^2$ is found. Starting from this minimum, perturbations in many directions (100 or more) are tested to find the boundary of the region within which $\chi^2 \le \chi^2_{min} + \chi^2_{limit}$. This boundary is used to define the uncertainty in the hotspot velocity magnitude and direction.

In typical chi-square analysis constraining parameters to measured values, the limiting value $\chi^2_{limit} = X^2_k(P)$, where $X^2_k$ is the inverse function of the cumulative chi-square distribution with $k$ degrees of freedom and $P$ is the desired probability

that the bound contains the true value. In this application, only a small number of measurements are used, comparable to the number of free parameters being fit (3). Moreover, the measurements are correlated: the NTOF detector positions are not perpendicular, and constraint on the velocity is relaxed in directions that are close to perpendicular from all the detectors. A numerical study was performed to confirm the appropriate value of $\chi^2_{limit}$ under these conditions. In this study, random velocity vectors were generated with a flat distribution in the ranges $0 \le V \le 200$ km/s, $0° \le \theta \le 180°$, and $0° \le \phi \le 360°$. One thousand "measurements" of each velocity were performed along each detector line-of-sight, including errors selected from a Gaussian distribution with a typical width (14 km/s). For each measurement, the $\chi^2$ metric was calculated for the true velocity and the best-fit velocity, and the distribution of the difference between these two values was calculated to determine the probability $P(\chi^2)$ that the original velocity vector was within $\chi^2_{limit}$ of the minimum $\chi^2$. A limiting value of $\chi^2_{limit} = 3.45 \pm 0.11$ was found to represent a $1\sigma$ uncertainty in the velocity ($P = 68\%$), and $\chi^2_{limit} = 7.75 \pm 0.31$ was found to represent a $2\sigma$ uncertainty ($P = 95\%$). These values are in agreement with the expected values, $X^2_3(0.68) = 3.51$ and $X^2_3(0.95) = 7.81$.

The shape of the uncertainty volume in velocity space is determined using this metric and the existing NIF detector positions and uncertainties, as shown in Fig. 3. The uncertainty is elongated in the direction (79°, 67°) that is least constrained by the existing detector lines of sight. This direction $\hat{v}$ has the minimum value of the quantity $\left[\sum_i (\hat{v} \cdot \hat{r}_i)^2\right]^{1/2}$, approximately one third of the maximum value. If the SPEC-E or SPEC-A detector is not included in the evaluation, the velocity cannot be accurately constrained along one axis.

The uncertainty in hotspot velocity is propagated into the NAD data by assessing the ensemble of acceptable corrections established by the uncertainty boundary. The activation data are renormalized using each boundary velocity point to produce an ensemble of corrected data. Spherical harmonic fits using modes 1 and 2 are applied to each of these corrected datasets, and the ensemble of fits is tested to define the uncertainty in the fits due to velocity correction.

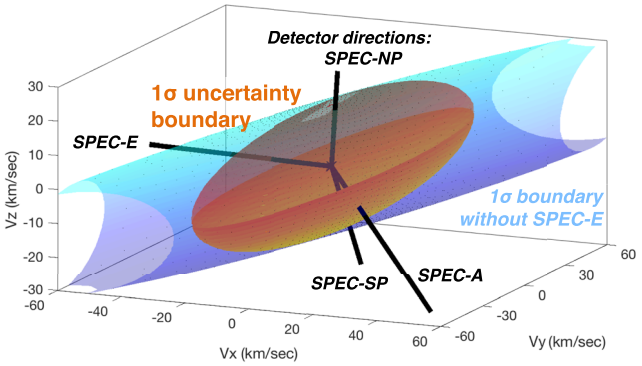


FIG. 3. Typical uncertainty volume (orange) for hotspot velocity inferred using the NIF NTOF detector positions (black lines). The boundary in hotspot velocity space is defined by $\chi^2 \le \chi^2_{min} + \chi^2_{limit}$, in which $\chi^2_{limit} = 3.45$ from a numerical study. If either the SPEC-E or SPEC-A detector is not included, the velocity is not constrained along one axis (without SPEC-E, blue).

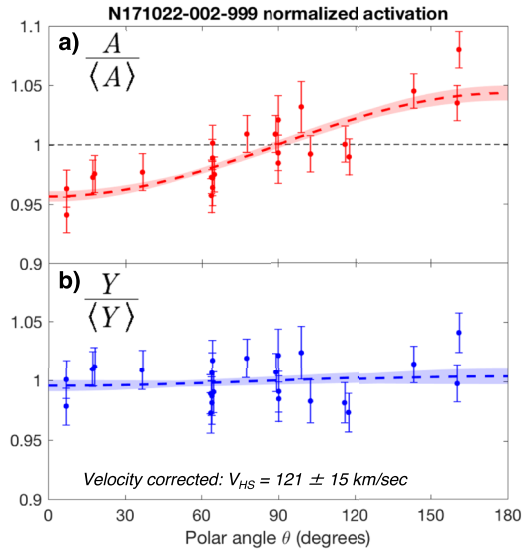


FIG. 4. Projection of (a) uncorrected and (b) velocity-corrected NAD data (points) from NIF Symcap shot N171022-002-999. Polar mode-1 fits (dashed lines) had amplitudes of −4.3% ± 0.5% before and −0.4% ± 0.6% after correction; uncertainty ranges are shaded.

## IV. EXPERIMENTAL RESULTS

A recent NIF implosion with an intentionally imposed mode-1 drive asymmetry (N171022-002-999) provides a valuable experimental test for the velocity correction. This gas-filled capsule implosion had low areal density at bang time: interpreting the downscattered neutron ratio as the fuel areal density, a value of $\langle \rho R \rangle = 83 \pm 28$ mg/cm$^2$ is inferred. Any areal density asymmetry will be comparably small ($Y/\langle Y \rangle - 1 \ll 1$), and the large imposed velocity should account for the majority of asymmetry in the activation signal. Using the methodology described in Sec. III, a hotspot velocity of $V_{HS} = 121 \pm 15$ km/s was observed, consistent with flow directly toward the south pole of the NIF target chamber ($\theta = 177°[+3, -12]$). Qualitatively, the uncorrected activation data also present a strong mode-1 perturbation toward the south pole, which is expected based on the velocity effects discussed in Sec. II; this result is shown in Fig. 4(a). A mode-1 fit to the uncorrected data has an asymmetry magnitude of −4.3% ± 0.5%. After applying the velocity correction [Fig. 4(b)], the magnitude of the mode-1 asymmetry is reduced to −0.4% ± 0.6%, indicating that the velocity correction accounts for the entire observed asymmetry in this case, as expected.

## V. CONCLUSIONS

In summary, a method for correcting $^{90}$Zr$(n,2n)^{89}$Zr nuclear activation data recorded on the NIF for the effects of hotspot velocity has been developed. The effect of mean hotspot velocity on activation is calculated due to three related effects: Doppler shift in the neutron spectrum, kinematic focusing of the neutron fluence in the direction of flow, and

change in the scattering cross section due to the Doppler shift. These three effects each amplify the activation by a factor proportional to the projection of the hotspot velocity onto the detector's line-of-sight. The residual signal of interest, which includes changes in local fluence due to variations in fuel $\rho R$, was recovered by renormalizing the measured activations to the value predicted, given a hotspot velocity. The magnitude and uncertainty of the mean hotspot velocity were inferred from NTOF diagnostics, and the appropriate chi-square boundary for propagating the measured uncertainty was evaluated numerically for the present system. This velocity correction method was applied to an implosion with imposed drive asymmetry and low residual areal density: the correction accounted for the observed polar activation asymmetry, demonstrating the accuracy of the technique. This technique provides a rigorous method to recover information on the three-dimensional hotspot and cold fuel assembly in cryogenic implosions on the NIF.

## ACKNOWLEDGMENTS

This work was performed under the auspices of the US Department of Energy by Lawrence Livermore National Laboratory under Contract No. DE-AC52-07NA27344 and supported in part by No. LDRD-17-ERD-060.

[1] D. S. Clark, A. L. Kritcher, J. L. Milovich, J. D. Salmonson, C. R. Weber, S. W. Haan, B. A. Hammel, D. E. Hinkel, M. M. Marinak, M. V. Patel, and S. M. Sepke, Plasma Phys. Controlled Fusion **59**, 055006 (2017).
[2] C. B. Yeamans and D. L. Bleuel, Fusion Sci. Technol. **72**, 120 (2017).
[3] C. J. Cerjan *et al.*, J. Phys. G: Nucl. Partic. **45**, 033003 (2018).
[4] B. K. Spears, M. J. Edwards, S. Hatchett, J. Kilkenny, J. Knauer, A. Kritcher, J. Lindl, D. Munro, P. Patel, H. F. Robey, and R. P. J. Town, Phys. Plasmas **21**, 042702 (2014).
[5] M. B. Chadwick *et al.*, Nucl. Data Sheets **107**, 2931 (2006).
[6] D. H. Munro, Nucl. Fusion **56**, 036001 (2016).
[7] L. Ballabio, J. Källne, and G. Gorini, Nucl. Fusion **38**, 1723 (1998).
[8] V. Y. Glebov, T. C. Sangster, C. Stoeckl, J. P. Knauer, W. Theobald, K. L. Marshall, M. J. Shoup, T. Buczek, M. Cruz, T. Duffy, M. Romanofsky, M. Fox, A. Pruyne, M. J. Moran, R. A. Lerche, J. McNaney, J. D. Kilkenny, M. J. Eckart, D. Schneider, D. Munro, W. Stoeffl, R. Zacharias, J. J. Haslam, T. Clancy, M. Yeoman, D. Warwas, C. J. Horsfield, J.-L. Bourgade, O. Landoas, L. Disdier, G. A. Chandler, and R. J. Leeper, Rev. Sci. Instrum. **81**, 10D325 (2010).
[9] V. Y. Glebov, C. Forrest, J. P. Knauer, A. Pruyne, M. Romanofsky, T. C. Sangster, M. J. Shoup, C. Stoeckl, J. A. Caggiano, M. L. Carman, T. J. Clancy, R. Hatarik, J. McNaney, and N. P. Zaitseva, Rev. Sci. Instrum. **83**, 10D309 (2012).
[10] R. Hatarik, D. B. Sayre, J. A. Caggiano, T. Phillips, M. J. Eckart, E. J. Bond, C. Cerjan, G. P. Grim, E. P. Hartouni, J. P. Knauer, J. M. McNaney, and D. H. Munro, J. Appl. Phys. **118**, 184502 (2015).
[11] R. Hatarik *et al.*, "Using multiple neutron time of flight detectors to determine the hot spot velocity," Rev. Sci. Instrum. (these proceedings).
[12] Second-moment effects, such as RMS velocity $\langle V^2 \rangle$, will produce spectral broadening. Given the near linearity of the activation cross section near 14.1 MeV, spectral broadening has a negligible effect for NADs.